ANNALS OF PHYSICS: 50, 571–597 (1968)

Orbit Properties of the Isochronous Cyclotron Ring with Radial Sectors*

M. M. GORDON

Cyclotron Laboratory, Michigan State University, East Lansing, Michigan 48823

The isochronous cyclotron considered here consists of a ring of radial magnet sectors separated by straight sections. The general features of such cyclotrons are discussed, and a complete analysis is presented of their orbit properties using the hard-edge approximation. This analysis proceeds through the transfer matrix technique, which is simplified by the symmetry of the magnet structure; the only complication arises from the inconstancy of the magnetic field index resulting from the isochronism condition. Computed orbit properties are presented and discussed for a wide variety of possible geometries; these properties include the extreme values of the beam widths, as well as the focusing frequencies, as a function of the energy. Problems associated with certain resonances are also considered. The results indicate that isochronous cyclotrons of this type should be quite capable of producing proton beams at energies up to about 500 MeV.

I. INTRODUCTION

Construction of an isochronous cyclotron in the form of a "ring", somewhat like a synchrotron, is not a novel concept. Indeed, an Isochronous Cyclotron Ring with spiralled sectors which will accelerate protons from 70 to 500 MeV, is now being constructed at ETH in Zurich (*1*). The present paper considers the simplest form of such accelerators, the Isochronous Cyclotron Ring with radial sectors. This simplicity manifests itself both in the constructional features of these cyclotrons, and in the analysis of the orbit properties.

The Isochronous Cyclotron Ring with radial sectors consists of N identical magnets each having a constant angular width $\Delta\theta$ corresponding to a "magnet fraction" $f = N(\Delta\theta)/2\pi$. The ring has an inner radius and an outer radius corresponding to the chosen energy range. Fig. 1 shows schematically a four-sector magnet geometry with each magnet having $\Delta\theta = 45°(f = 0.5)$ and with inner and outer radii chosen to correspond to a 20–200 MeV energy range. Similarly, Fig. 2 shows a six-sector geometry with $\Delta\theta = 18°(f = 0.3)$ corresponding to a 20–500 MeV energy range. In both cases the inner radius, and hence the injection energy,

* This work has been supported by the National Science Foundation, partly at Indiana University.

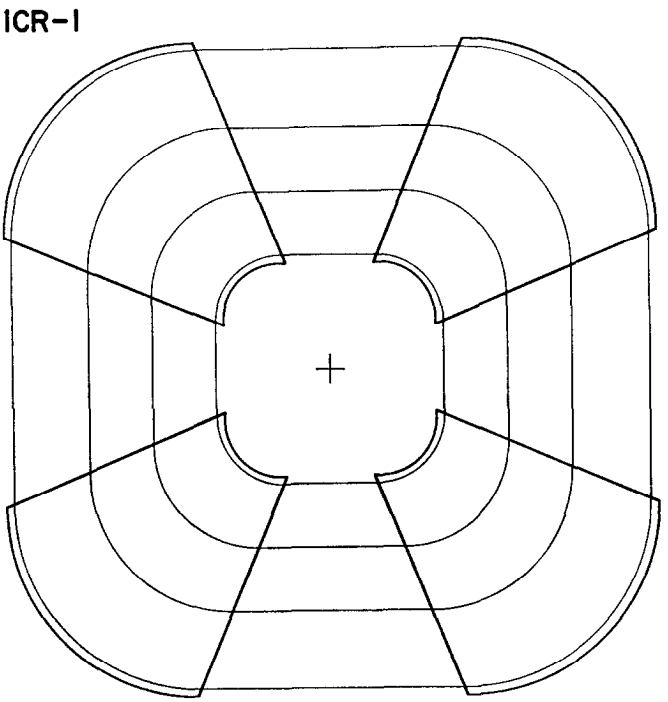

FIG. 1. Four-sector isochronous cyclotron ring with magnets having constant angular width $\Delta\theta = 45°$ (magnet fraction, $f = 0.5$). The orbits which are shown correspond to the following proton energies: 20, 50, 100, and 200 MeV.

has been chosen rather arbitrarily; in actual practice, this choice must be based on a variety of engineering considerations. For the machines depicted in Figs. 1 and 2, a low energy ring of similar construction could be used to produce the 20 MeV beam required for injection.

Since the radiofrequency structures (dees or cavities) would be situated in the "valleys" between the magnets (straight sections), the magnet gaps could be quite small. The use of narrow gap magnets substantially improves the vertical focusing properties of these magnets. Assuming flat pole-faces, then all the important surfaces of each magnet would be flat surfaces, which greatly simplifies the construction of these magnets even when they are very large. Each magnet, together with its coils and pole-face windings, could be constructed separately and then properly assembled into the ring. Since ample space is available in the straight sections, it should be possible for the radiofrequency accelerating system to produce a large energy gain per turn. Alternate straight sections could be used for the rf system operating at the main frequency, with the remaining straight sections occupied by

a third harmonic rf system designed to produce a "flat-top" on the effective voltage wave form; such a design could yield separated turns together with a considerable increase in the duty factor (*2*). Since this third harmonic system would be relatively small, the same straight sections which it occupies could also be used for beam injection and beam extraction.

The Isochronous Cyclotron Ring requires an injected beam obtained from an external ion source or from a lower energy ring. The use of a ring geometry for the lowest energy stage eliminates the central region problems associated with the conventional cyclotron, which stem from the weak vertical focusing and from the constraints imposed by an internal ion source. The external source required for the ring permits the tailoring of the properties of the injected beam so as to match most effectively the transmission characteristics of the machine. In addition, the beam injection system for the ring can quite readily be adapted for use with a source

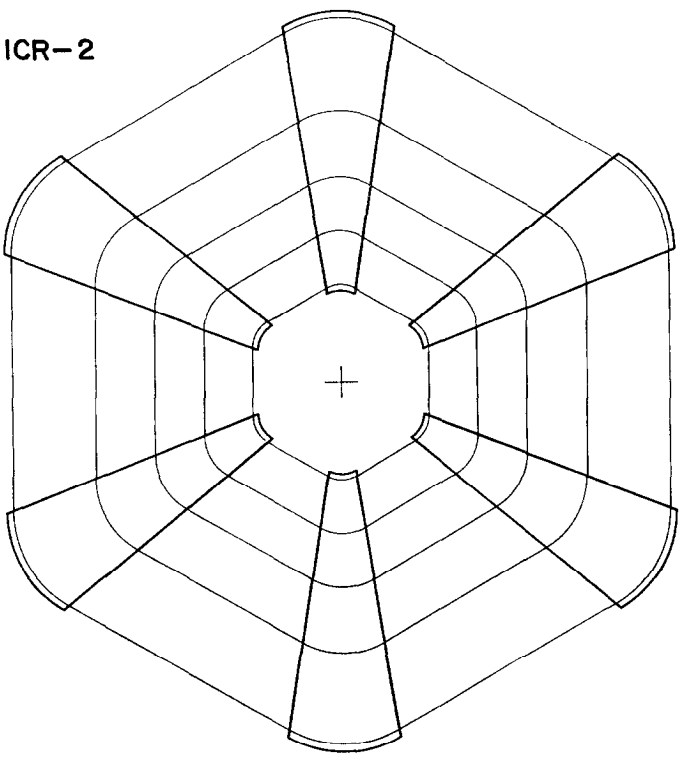

FIG. 2. Six-sector isochronous cyclotron ring with magnets having constant angular width $\Delta\theta = 18°$ (magnet fraction, $f = 0.3$). The orbits which are shown correspond to the following proton energies: 20, 50, 100, 200, and 500 MeV.

of polarized ions. Finally, the presence of straight sections in the ring greatly simplifies the problem of beam injection.

As shown in Figs. 1 and 2, each equilibrium orbit consists of circular arc segments within the magnets joined by straight line segments in the valleys. Thus, it is assumed that the angular width of the magnet edge region, within which the magnetic field falls off to zero, is negligibly small compared with the angular width of either the magnet or the valley (hard-edge approximation); this is a reasonable approximation for the small magnet gaps considered here. For a fixed orbital frequency the velocity v is proportional to the radius of curvature ρ of the circular arc; as a result, the fixed inner and outer radii of a given geometry specify only the ratio v_f/v_i where v_i and v_f are the initial and final velocities of the particle. For example, the four-sector geometry depicted in Fig. 1, which was chosen for a 20–200 MeV energy range, could just as well be used for a 2.6–20 MeV energy range. The orbit geometry is clearly the same at all energies except for a scale factor. Moreover, this geometry is independent of the orbital frequency and would therefore remain the same if the final energy or the accelerated ion were changed.

The magnetic field B is constant along the circular arc segments of each equilibrium orbit. Thus, each of these circular arcs represents an iso-gauss contour line, and the pole-face windings used to produce the desired field variation should be shaped accordingly. Since the orbit geometry is invariant under a change of orbital frequency, the same set of pole-face windings should be applicable under all operating conditions. To satisfy the isochronism condition, the value of B along a given circular arc must be proportional to the corresponding value of γ, the relativistic mass factor; a sufficient number of pole-face windings must be provided so as to produce this required field variation with reasonable accuracy. If γ_i and γ_f are the initial and final values of γ over the energy range of the ring, then γ_f/γ_i specifies the ratio of maximum to minimum values of B which must be produced within the ring. For example, for the 20–200 MeV ring depicted in Fig. 1, this ratio is about 1.2 which seems quite feasible; however, for the 20–500 MeV ring depicted in Fig. 2, the field ratio is about 1.5 which may be difficult to achieve in practice. The 20–500 MeV machine could be built in two stages with the first stage going to, say, 200 MeV; although the required field variation would be easier to produce in each ring, such a design is faced with the difficult problem of extracting the 200 MeV beam from the first stage and injecting this beam into the second stage.

All the properties of the horizontal and vertical linear oscillations, such as the focusing frequencies and the beam widths, as a function of the energy depend only on the number of sectors N and the magnet fraction f characterizing the geometry. Because of the isochronism condition, the vertical focusing frequency ν_z decreases with energy; however, since $\nu_z \cong [(1/f) - 1]^{1/2}$ at $E = 0$, for values of f between

0.2 and 0.5, the initial value of ν_z is sufficiently large so that the vertical focusing remains quite good over a substantial energy range. Actually, as will be seen in Section VI, the variation of the maximum beam width as a function of energy provides a proper criterion for the adequacy of the vertical focusing. Because of the problems encountered with various resonances, for a given value of N, certain values of f must be excluded from consideration, while for other f values the feasible energy range must be restricted. The four-sector geometry shown in Fig. 1 with $f = 0.5$ posesses exceptionally good orbit properties and avoids serious resonance problems over the entire proton energy range up to about 300 MeV; the same can be said for the six-sector geometry, depicted in Fig. 2, with $f = 0.3$ for all proton energies up to about 500 MeV. Many other geometries also posess very favorable orbit properties, and all deserve serious consideration.

II. GEOMETRY AND ISOCHRONOUS FIELD

Because of the symmetry of the magnet configuration, consideration is required of only one-half of a sector for a complete analysis of the properties of the equilibrium orbits and their associated linear oscillations. Figure 3 exhibits the geometry of the half sector upon which the analysis is based. The magnetic field extends from $\theta = 0$, the center of the magnet, to $\theta = \alpha$, the edge of the magnet, at which point the field is assumed to drop abruptly to zero; from $\theta = \alpha$ to $\theta = \delta$, the center of the valley, the field is therefore zero. If $\Delta\theta$ is the constant angular width of the magnet, and if f is the magnet fraction defined in the preceding section, then:

$$\delta = \pi/N, \qquad \alpha = (\Delta\theta)/2 = f\delta. \tag{1}$$

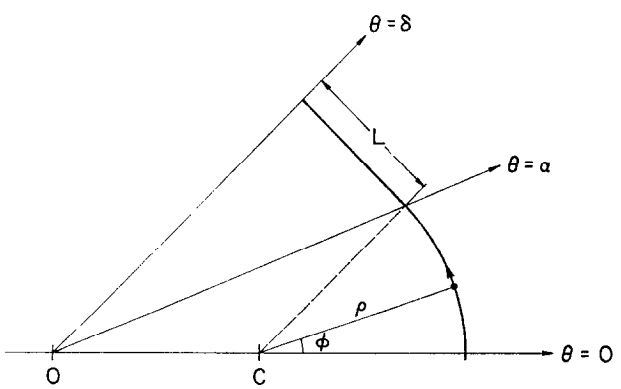

FIG. 3. Geometry for one-half of a sector, from the center of a magnet to the center of a valley, showing the equilibrium orbit and the various parameters describing this geometry.

The portion of the equilibrium orbit (EO) shown in Fig. 3 consists of a circular arc segment of constant radius of curvature ρ from $\theta = 0$ to $\theta = \alpha$, and a straight line segment of length L from $\theta = \alpha$ to $\theta = \delta$. The point C is the center of the circular arc segment of the EO, and the distance from the origin O (machine center) to the point C is given by:

$$OC = b\rho, \tag{2a}$$

$$b = (\sin(\delta - \alpha))/(\sin \alpha). \tag{2b}$$

The angle ϕ shown in Fig. 3 constitutes a polar angle relative to the point C, and specifies the position of the particle along the EO within the magnet; thus, $\phi(\theta = 0) = 0$ and $\phi(\theta = \alpha) = \delta$. The length of the circular arc portion of the EO shown in Fig. 3 is $\rho\delta$, so that the length L of the straight line segment can be specified by the parameter a as follows:

$$L = a(\rho\delta), \tag{3a}$$

$$a = b(\sin \delta)/\delta. \tag{3b}$$

Thus, if f_0 is the fraction of the arc length of the EO which is within the magnet, then:

$$f_0 = (1 + a)^{-1} = f[1 + (1/3)(1 - f)^2 \delta^2 + \cdots], \tag{4}$$

where the second expression represents an expansion in powers of δ^2.

An arc length variable s is introduced such that $s = \rho\phi$ within the magnet; thus, $s = 0$ at the center of the magnet, $s = s_0$ at the edge of the magnet, and $s = s_1$ at the center of the valley, where:

$$\begin{aligned} s_0 &= \rho\delta, \\ s_1 &= \rho\delta + L = \rho\delta(1 + a). \end{aligned} \tag{5}$$

It follows then that the total arc length of the EO around the machine is given by:

$$2Ns_1 = 2\pi\rho/f_0 = vT, \tag{6a}$$

where v is the velocity of the particle and T is its period of rotation. Setting $2\pi/T = f_0\omega$, then:

$$v = \rho\omega, \tag{6b}$$

where ω is the constant angular velocity of the particle within the magnet relative to the point C in Fig. 3.

If the magnetic field B is perfectly isochronous, then T, and hence ω, is a constant

independent of the energy of the particle. In this case, the value of B along the circular arc segment of the EO is given by:

$$B(\rho) = (m_0\omega/q)\gamma, \tag{7a}$$

where m_0 and q are the rest mass and charge of the ion, and γ is given by:

$$\gamma = (1 - \beta^2)^{-1/2}, \tag{7b}$$

with $\beta = v/c$. This then is the isochronous magnetic field, and it should be noted that the circular arcs which form the iso-gauss contours for this field are not concentric. If ω_{rf} is the circular RF frequency, then $\omega_{rf} = 2\pi h/T = h\omega f_0$, where h is the integral harmonic ratio.

III. LINEAR MOTION

The displacement of the particle from the EO is described by the coordinates $x(s)$ and $z(s)$ where s is the arc length along the EO. The vertical coordinate z represents the displacement perpendicular to the median plane. The horizontal coordinate x represents a displacement in the median plane in the direction of the outward normal to the EO at the given value of s; this definition of x coincides with the one customarily used in synchrotron orbit analyses. We depart from customary practice by employing the conjugate momenta p_x and p_z rather than (dx/ds) and (dz/ds), where:

$$p_x = p(dx/ds), \qquad p_z = p(dz/ds); \tag{8}$$

although this change is a minor one, it has the advantage of making phase space consequences (via Liouville's theorem) completely transparent. We also adopt "modified cyclotron units" wherein the momenta p_x, p_z, and p have units of length the same as x, z, and ρ; that is, for example,

$$p = (\beta\gamma)(c/\omega) = \rho\gamma, \tag{9}$$

as follows from Eqs. (6,7). This convention has the advantage of rendering the transfer matrices dimensionless.

Within the magnet the coordinate system corresponds to cylindrical polar coordinates centered at the point C of Fig. 3; the position of the particle is specified by the variables $(\rho + x, \phi, z)$ relative to this point. In order to calculate orbit properties, the median plane field B of Eq. (7) must be expressed in terms of the variables x and ϕ, bearing in mind that the origin C of this coordinate system changes with the energy of the particle. Consider the point P with coordinates

$(\rho + x, \phi)$ relative to the point C; the point P lies on a different circular iso-gauss contour the center of which is at the point C', such that the distance $C'P = \rho'$, and the distance $OC' = b\rho'$ (cf. Eq. (2)). Considering then the triangle CPC', it follows that:

$$(\rho')^2 = (\rho + x)^2 + b^2(\rho' - \rho)^2 - 2b(\rho' - \rho)(\rho + x)\cos\phi, \tag{10}$$

so that $\rho' = \rho$ for $x = 0$. This equation can readily be solved for ρ' in terms of ρ, x, ϕ; the value of $B(\rho')$ at the point P is then given by Eq. (7) with ρ replaced by ρ'. For most analytical purposes, the value of B is expanded in powers of x; for example, to first order,

$$\begin{aligned} B(\rho') &= B(\rho) + x(dB/d\rho)(\partial\rho'/\partial x), \\ (\partial\rho'/\partial x) &= (1 + b\cos\phi)^{-1}, \end{aligned} \tag{11}$$

as follows from Eq. (10).

For linear oscillations about the EO, the key parameter is the field index k defined by: $k = (\rho/B)(\partial B/\partial x)$. Upon using Eq. (11) this becomes:

$$k(\phi) = (\beta\gamma)^2(1 + b\cos\phi)^{-1}, \tag{12}$$

since B is proportional to γ, and ρ is proportional to β as given in Eqs. (6, 7). Thus, k is a function of ϕ, and is smaller than $(\beta\gamma)^2$ to which it reduces when $f = 1$, that is, when the magnet occupies the complete sector. The value of k obtained from Eq. (12) applies, of course, only within the magnet; that is, from $\phi = 0$ to $\phi = \delta$, in the half sector under consideration here.

The differential equations for the linear oscillations about the EO within the magnet are:

$$(d^2x/d\phi^2) + [1 + k(\phi)]x = 0, \tag{13a}$$

$$(d^2z/d\phi^2) - k(\phi)z = 0, \tag{13b}$$

where $k(\phi)$ is given by Eq. (12). In order to construct the transfer matrices, two linearly independent solutions of each of these equations are required over the range: $s(\phi = 0) = 0$ to $s(\phi = \delta) = s_0$, that is, from the center to the edge of the magnet. Approximate solutions of these differential equations will be discussed in Section V; however, the structure of these equations is sufficiently simple to make them quite amenable to numerical solution with a digital computer. Note that within the magnet $p_x = \gamma(dx/d\phi)$ and $p_z = \gamma(dz/d\phi)$ as follows from Eqs. (8, 9) in the units adopted here.

At the edge of the magnet ($s = s_0$) the field drops abruptly to zero, and in this "hard-edge" approximation the values of p_x and p_z change discontinuously

at this point (*3*). From the orbit geometry depicted in Fig. 3, it follows that the field index at the magnet edge is given by:

$$k_{\text{edge}} = -\tan(\delta - \alpha)\, \Delta(\phi - \delta), \tag{14a}$$

where $\Delta(\phi - \delta)$ is a Dirac delta function. It then follows from Eq. (13) that the impulsive change in p_x and p_z at the magnet edge is given by:

$$\Delta p_x(s_0) = +\gamma t x(s_0), \tag{14b}$$

$$\Delta p_z(s_0) = -\gamma t z(s_0), \tag{14c}$$

where the symbol t stands for:

$$t = \tan(\delta - \alpha). \tag{15}$$

This change in p_z can be recognized as the "edge focusing" arising from the field component B_θ at the magnet edge. A particle with positive x actually arrives at the magnet edge "early" so that its momentum vector rotates through a smaller angle than for the EO; thus, the change Δp_x simply compensates for the extra rotation and does not constitute, therefore, any actual defocusing at the magnet edge.

From the edge of the magnet at $s = s_0$ to the center of the valley at $s = s_1$, the magnetic field is identically zero so that the values of p_x and p_z do not change in this region. Thus, the values of the orbit coordinates and momenta at the center of the valley are given by:

$$\begin{aligned} p_x(s_1) &= p_x(s_0) + \gamma t x(s_0), \\ x(s_1) &= (1 + ta\delta)\, x(s_0) + (a\delta/\gamma)\, p_x(s_0), \\ p_z(s_1) &= p_z(s_0) - \gamma t z(s_0), \\ z(s_1) &= (1 - ta\delta)\, z(s_0) + (a\delta/\gamma)\, p_z(s_0), \end{aligned} \tag{16}$$

where the values at $s = s_0$ are obtained from the solutions of Eq. (13), and where $L/p = (a\delta/\gamma)$ following Eqs. (3, 9). Thus, the phase space vectors (x, p_x) and (z, p_z) can be traced from the center of the magnet to the center of the valley, thereby completing the description of these vectors over the required half sector. As will be seen in the next section, this information is sufficient to determine the linear oscillation properties throughout the complete sector.

IV. TRANSFER MATRIX PROPERTIES

In this section (y, p_y) will be used to stand for either (x, p_x) or (z, p_z) whenever a given relation applies equally well to both. If the phase space vector (y, p_y) is represented by the column matrix $Q(s)$, then following Courant and Snyder (*4*),

the transfer matrix $M(s)$ for one sector ($\Delta s = 2s_1$) starting at the point s is defined by:

$$Q(2s_1 + s) = M(s)\, Q(s). \tag{17a}$$

This transfer matrix is written as follows:

$$M(s) = I \cos \mu + J(s) \sin \mu; \tag{17b}$$

where I is the unit matrix, and

$$\mu = \nu_y(2\pi/N) = 2\nu_y\delta; \tag{17c}$$

$$J(s) = \begin{pmatrix} \alpha(s) & \beta(s) \\ -\gamma(s) & -\alpha(s) \end{pmatrix}. \tag{17d}$$

The quantity ν_y is the focusing frequency; the quantities $\alpha(s)$, $\beta(s)$, $\gamma(s)$ are periodic functions of s with periodicity equal to one sector, and satisfy the following relation:

$$\beta(s)\,\gamma(s) = 1 + \alpha^2(s). \tag{18}$$

In order to avoid confusion, the α, β, γ used in the preceding sections will not be used at all in this section, while the $\alpha(s)$, $\beta(s)$, $\gamma(s)$ introduced here will appear only in this section. Note that $\alpha(s)$, $\beta(s)$, $\gamma(s)$ are all dimensionless in the units adopted here; using the subscript "c" to designate the same quantities as used by Courant and Snyder, then the following relations hold: $\alpha_c = \alpha$; $\beta_c = p\beta$; $p\gamma_c = \gamma$.

Suppose that the transfer matrix $M(s)$ is repeatedly applied to the vector $Q(s)$, then the sequence of phase space points $(y,\ p_y)$ so generated will lie on an ellipse whose equation is given by:

$$\gamma(s)\, y^2 + \beta(s)\, p_y^2 + 2\alpha(s)\, y p_y = A^2, \tag{19}$$

where A is a constant independent of s. This "eigen-ellipse" is characteristic of the given point s in the sector, and is determined by the values of the periodic functions α, β, γ at this point. The area of this ellipse is πA^2, so that if the ellipse is examined at different values of s, its eccentricity and orientation may change, but not its area. Upon differentiating Eq. (19), the maximum values of y and p_y are found to be:

$$\begin{aligned} [y(s)]_{\max} &= A[\beta(s)]^{1/2}, \\ [p_y(s)]_{\max} &= A[\gamma(s)]^{1/2}. \end{aligned} \tag{20}$$

Consider now a beam of particles all at the same energy E, and suppose that their

(y, p_y) phase space points at the given value of s completely fill the eigen-ellipse given by Eq. (19); that is, the ith particle has $A_i \leqslant A$. It follows then that the "widths" Δy and Δp_y for the entire beam of particles are given by:

$$\Delta y = 2A[\beta(s, E)]^{1/2}, \tag{21a}$$

$$\Delta p_y = 2A[\gamma(s, E)]^{1/2}, \tag{21b}$$

and since A is constant, these relations determine the widths as a function of s. Now the area πA^2 is an invariant, and under conditions of adiabatic acceleration, the relations (21) specify the variation of the beam widths as a function of the energy E as well as the position s. These relations can be applied to any accelerated beam, and the value of the amplitude A can be determined from the smallest eigen-ellipse which completely encloses the phase space area occupied by the beam at injection (or anywhere else); obviously, for maximum efficiency the beam should completely fill the eigen-ellipse. Evidently, a knowledge of the widths $[\beta(s, E)]^{1/2}$ and $[\gamma(s, E)]^{1/2}$ as a function of s and E provides much more detailed information on the focusing produced by the magnet structure than does the focusing frequency ν_y ; the value of ν_y is important mainly in determining the location of various resonances. It should be noted that Liouville's theorem requires only that the phase space area occupied by the beam remain constant; on the other hand, the assumptions of linearity (including the absence of resonances) and adiabaticity together specify in detail the nature and evolution of this phase space area throughout the machine. It should also be noted that the functions β and γ, as defined here, already contain all the "adiabatic damping" factors.

Suppose that at the given energy E, two independent solutions (y_1, p_{y1}) and (y_2, p_{y2}) are obtained for the linear equations of motion over one complete sector from $s = 0$ to $s = 2s_1$, with their initial conditions given by (1, 0) and (0, 1), respectively. Consider then the matrix $Y(s)$ formed from these solutions as follows:

$$Y(s) = \begin{pmatrix} y_1 & y_2 \\ p_{y1} & p_{y2} \end{pmatrix}; \tag{22a}$$

then, since $Y(0) = I$, the unit matrix, it follows that $Y(s)$ is the transfer matrix from $s = 0$ to a given s; that is,

$$Q(s) = Y(s)\, Q(0). \tag{22b}$$

Since the Hamiltonian is invariant under a displacement in s by one sector, it also follows that:

$$Q(s + 2s_1) = Y(s)\, Y(2s_1)\, Q(0), \tag{22c}$$

which, when compared with Eq. (17), yields the following equations:

$$M(0) = Y(2s_1); \tag{23a}$$

$$M(s) = Y(s)\, M(0)\, Y^{-1}(s); \tag{23b}$$

$$J(s) = Y(s)\, J(0)\, Y^{-1}(s). \tag{23c}$$

Thus, Eq. (23a) can be used to calculate the value of ν_y (within limits) as well as the values of $\alpha(0)$, $\beta(0)$, and $\gamma(0)$; then, Eq. (23c) can be used to calculate α, β, and γ at all other s values for the complete sector.

The time reversal operator T can be represented by the following matrix:

$$T = \begin{pmatrix} 1 & 0 \\ 0 & -1 \end{pmatrix} = T^{-1}, \tag{24a}$$

which has the effect of replacing p_y by $-p_y$ while leaving y unchanged. For the symmetric magnet geometry being considered here, the Hamiltonian is invariant under reflection in s about any symmetry point such as $s = 0$ (the center of a magnet "hill"), or $s = s_1$ (the center of a "valley"). This symmetry yields the following relations:

$$Q(s) = Y(s)\, Q(0) = TY(-s)\, TQ(0), \tag{24b}$$

$$Q(s + s_1) = Y(s + s_1)\, Y^{-1}(s_1)\, Q(s_1) = TY(s_1 - s)\, Y^{-1}(s_1)\, TQ(s_1), \tag{24c}$$

so that:

$$Y(-s) = TY(s)T, \tag{25a}$$

$$Y(s_1 + s) = TY(s_1 - s)\, Y^{-1}(s_1)\, TY(s_1). \tag{25b}$$

Hence, the solutions generated in the preceding section over half the sector from $s = 0$ to $s = s_1$ can thereby be extended to the remaining half of the sector.

From Eq. (23a) and Eq. (25b), it follows that:

$$M(0) = TY^{-1}(s_1)\, TY(s_1), \tag{25c}$$

which, upon evaluation and identification via Eq. (17), yields the following results:

$$\sin^2(\nu_y \delta) = -y_2(s_1)\, p_{y1}(s_1), \tag{26a}$$

$$\alpha_h = 0, \qquad \gamma_h = 1/\beta_h\,, \tag{26b}$$

$$(\beta_h)^2 = -[y_2(s_1)\, p_{y2}(s_1)]/[y_1(s_1)\, p_{y1}(s_1)], \tag{26c}$$

where the subscript "h" designates the value at the center of the hill ($s = 0$). From Eq. (23c) and the fact that $\alpha_h = 0$, it can also be shown that:

$$\beta(s) = \beta_h\, y_1^2(s) + \gamma_h y_2^2(s), \tag{27a}$$

$$-\alpha(s) = \beta_h\, y_1(s)\, p_{y1}(s) + \gamma_h\, y_2(s)\, p_{y2}(s), \tag{27b}$$

$$\gamma(s) = \beta_h\, p_{y1}^2(s) + \gamma_h\, p_{y2}^2(s). \tag{27c}$$

Further analysis provides the following symmetry relation for $J(s)$:

$$J(-s) = -TJ(s)T; \tag{28}$$

so that $\beta(s)$ and $\gamma(s)$ are both symmetric about any symmetry point, while $\alpha(s)$ is antisymmetric about such points; consequently, $\alpha = 0$ at any symmetry point. Thus, the values of α, β, γ need only be calculated for half of a sector because of this symmetry. The relations (26, 27, 28) will therefore permit the calculation of ν_y as well as the values of α, β, γ at any point in the sector from the given values of $Y(s)$ from $s = 0$ to $s = s_1$. In particular, for $s = s_1$ at the center of the valley, the following values are obtained:

$$\alpha_v = 0, \qquad \gamma_v = 1/\beta_v, \tag{29a}$$

$$(\beta_v)^2 = -[y_1(s_1)\ y_2(s_1)]/[p_{y1}(s_1)\ p_{y2}(s_1)], \tag{29b}$$

where the subscript "v" indicates the center of a valley. The foregoing relations are quite general in that they will apply to any symmetric magnet structure.

Since the quantity β specifies the beam width as a function of position and energy via (21a), it is of considerable importance to determine at which values of s this function has its maximum and minimum values. The derivatives of β are given by:

$$p(d\beta/ds) = -2\alpha(s), \tag{30a}$$

$$p(d\alpha/ds) = K(s)\,\beta(s) - \gamma(s), \tag{30b}$$

where $K_x = (p/\rho)^2(1 + k)$, and $K_z = -(p/\rho)^2 k$; these equations can be derived by differentiating the relations (27) and using the equations of motion. Thus, β has a maximum or minimum value wherever $\alpha = 0$. Moreover, since $\alpha = 0$ at each symmetry point ($s = 0$, $s = s_1$), then β must have an extremum at such points. In addition, β may have an extremum at the magnet edge ($s = s_0$) since the value of α is discontinuous at this point and may pass through zero. Using the subscript "e" to denote the value at the edge of the magnet, the discontinuity in α is given by:

$$\Delta\alpha_e = \pm(p/\rho)\, t\beta_e, \tag{31}$$

as can be seen from Eqs. (14, 27b), where the (+) sign applies to the z-motion, and the (−) sign to the x-motion. Since $K = 0$ in the valley, then Eq. (30b) shows that α must be positive following the magnet edge, and then decreased to zero at the center of the valley; as a result, β has a minimum value β_v at the center of the valley for both the x-motion and z-motion. Since $K_z < 0$ within the magnet, the value of α starts from zero at the center of the hill and decreases out to the magnet edge; thus, β_z must have a minimum value β_{zh} at the center of the hill. Therefore, β_z must have its maximum value β_{ze} at the magnet edge (this is consistent with the

fact that α_z from (31) increases across the magnet edge); the value of β_e is found to be:

$$\beta_e = \beta_v + (a\rho\delta/p)^2 (\beta_v)^{-1}, \tag{32}$$

from Eqs. (27a, 16) and $\alpha_v = 0$. Now Eq. (31) shows that α_x decreases at the magnet edge, and since it is positive beyond this point, then α_x must also be positive prior to the magnet edge, and β_x cannot have an extremum at this point; as a result, α_x must be positive for $0 < s < s_0$ (provided $\nu_x < N/2$), and β_x must have a maximum value β_{xh} at the center of the hill. Introducing the width function W,

$$W(s, E) = [\beta(s, E)]^{1/2}, \tag{33}$$

the foregoing conclusions can be summarized as follows: for the x-motion, W_x has its maximum value W_{xh} at the center of a hill and decreases continuously to its minimum value W_{xv} at the center of a valley; for the z-motion, W_z has a minimum value W_{zh} at the center of a hill, rises to its maximum value W_{ze} at the magnet edge, and then decreases to a second minimum value W_{zv} at the center of a valley; that is,

$$W_{\max} = W_{xh}, W_{ze}; \tag{34a}$$

$$W_{\min} = W_{xv}, W_{zh}, W_{zv}. \tag{34b}$$

The values of W_{xh}, W_{zh}, W_{xv}, and W_{zv} can be calculated from the corresponding values of β_h and β_v obtained from Eqs. (26c, 29b); the value of W_{ze} can then be calculated using Eq. (32).

The beam "divergence" width Δp_y is determined by the quantity γ as a function of position and energy as can be seen from Eq. (21b). The derivative of γ is given by:

$$p(d\gamma/ds) = 2K(s)\,\alpha(s), \tag{35}$$

as obtained by differentiating (27c), and where K is given following (30). From the foregoing discussion, it can be concluded that $(d\gamma/ds) > 0$, for $0 < s < s_0$, for both the x-motion and the z-motion; it therefore follows that γ has a minimum value $\gamma_h = 1/\beta_h$ at the center of the hill in both cases. Within the valley, γ has a constant value $\gamma_v = 1/\beta_v$ for both cases. For the x-motion, $|\alpha_x|$ decreases at the magnet edge so that γ_x has its maximum value γ_{xe} just prior to this point. For the z-motion, the value of γ_z may either increase or decrease at the magnet edge depending on whether $|\alpha_z|$ increases or decreases at this point.

V. APPROXIMATE SOLUTIONS

In order to obtain approximate solutions of the differential equations (13), it should be noted that $k(\phi)$ varies quite slowly over the ϕ range of interest $0 \leqslant \phi \leqslant \delta$, particularly if N is large. As a consequence, a simple approximation

can be obtained by replacing $\cos \phi$ in the expression (12) by its average value: $\langle \cos \phi \rangle = (\sin \delta)/\delta$. In this case, $k(\phi)$ becomes equal to a constant:

$$k(\phi) \rightarrow k_0 = f_0(\beta\gamma)^2, \tag{36}$$

where f_0 is given by Eq. (4). This approximation simplifies the differential equations (13) such that their solutions become either circular or hyperbolic functions. The WKBJ approximation would, of course, yield improved results; however, the amount of this improvement does not warrant the extra complexity.

The solutions of the differential equations provide the matrix elements of $Y(s)$, as defined in (22) over the range $0 < s < s_0$. The elements of $Y(s_1)$ can then be obtained from Eq. (16). The values of ν_y can then be calculated from Eq. (26a); the beam widths given in (34) can be calculated by the procedure described thereafter. The approximate results so obtained have an error which can be shown to vary as $(1 - f)^2/N^4$; furthermore, although these results are exact for $E = 0$, the error increases with energy. The values of ν_x, ν_z, and the W's of (34) obtained from this approximation have been compared with more accurate values obtained by numerical integrations with the following results (cf. Tables III and IV): (a) for $N = 4$ and $f = 0.5$, the error in all quantities is less than 0.1 % for $E < 0.10$, less than 0.5 % for $E < 0.27$, and less than 1 % for $E < 0.34$; (b) for $N = 6$ and $f = 0.3$, the error is less than 0.1 % for $E < 0.43$, less than 0.5 % for $E < 0.73$, and less than 1 % for $E < 0.80$.

In order to obtain explicit, simple formulas, the above approximation can be pursued to its ultimate limit: $\delta \rightarrow 0 (N \rightarrow \infty)$. (This limiting case is similar to the so-called "smooth approximation".) In this limit, the following results are obtained:

$$\nu_{x0} = \gamma; \tag{37a}$$

$$(\nu_{z0})^2 = f^{-1} - \gamma^2; \tag{37b}$$

$$W_{y0} = (f\gamma\nu_y)^{-1/2}; \tag{37c}$$

where the width function W_{y0} is a constant independent of s in this approximation. These results work best when $(1 - f)$ is small and when $\nu_y \ll N/2$. These simple equations provide a true indication of the dependence of ν_y and W_y on the value of f and the energy E. It may be noted that the values of ν_{x0} and ν_{z0} are always smaller than the actual values.

In the nonrelativistic limit ($E \rightarrow 0$) the field within the magnets is constant so that $k = 0$. Simple analytical results can again be obtained in this case and although these results are strictly valid only for $E = 0$, they will be reasonably accurate for low energy cyclotrons. In particular, this approximation yields the following equations for ν_x and ν_z:

$$\sin(\nu_x\delta) = (\sin \delta)/(\cos(\delta - \alpha)); \tag{38a}$$

$$\cos^2(\nu_z\delta) = (1 - t\delta)(1 - at\delta); \tag{38b}$$

where $t = \tan(\delta - \alpha)$. An examination of (38a) reveals that for $f < f_m$, the value of ν_x falls in the $N/2$ stop-band; the value of f_m is given by:

$$f_m = (4 - N)/2. \tag{39}$$

Since the value of ν_x increases with energy, the restriction $f > f_m$ must hold for all energies. For $N = 2$, the value $f_m = 1$ shows that ν_x always lies in the stop-band, so that $N = 2$ must be ruled out (this is generally true for any isochronous cyclotron with an azimuthally varying field); for $N = 3$, only $f > 0.5$ is permissible; for $N \geqslant 4$, this consideration places no restriction on the possible f values. Analysis of Eq. (38b) shows that for $f < f'_m$, the value of ν_z will lie in the $N/2$ stop-band; the following formula can be used to determine f'_m:

$$\tan(2f'_m\delta) = 2(\tan^3 \delta)/(1 + 3 \tan^2 \delta). \tag{40}$$

This consideration produces the following restrictions: for $N = 3$, $f > 0.384$ ($< f_m = 0.5$); for $N = 4$, $f > 0.295$; for $N = 6$, $f > 0.182$; and for large N values, $f > \delta^2(1 + \delta^2)/(1 + 3\delta^2)$. Since ν_z decreases with energy, the restriction $f > f'_m$ does not hold at all energies for f'_m given above; however, values of

TABLE I

NON-RELATIVISTIC LIMITS ($E = 0$)

	$N = 3$		$N = 4$		$N = 6$		$N = \infty$
f	ν_x	ν_z	ν_x	ν_z	ν_x	ν_z	ν_z
0.90	1.009	0.339	1.004	0.336	1.002	0.335	0.333
0.85	1.021	0.429	1.009	0.425	1.003	0.422	0.420
0.80	1.038	0.514	1.016	0.507	1.006	0.503	0.500
0.75	1.062	0.596	1.025	0.587	1.010	0.581	0.577
0.70	1.093	0.679	1.037	0.667	1.014	0.660	0.655
0.65	1.135	0.765	1.051	0.749	1.019	0.740	0.734
0.60	1.191	0.855	1.067	0.835	1.025	0.824	0.817
0.55	1.273	0.952	1.087	0.927	1.032	0.914	0.905
0.50	1.500	1.060	1.110	1.029	1.039	1.012	1.000
0.45	*****		1.136	1.146	1.048	1.122	1.106
0.40			1.167	1.287	1.057	1.250	1.225
0.35			1.203	1.475	1.068	1.404	1.363
0.30			1.245	1.840	1.079	1.600	1.528
0.25				*****	1.092	1.877	1.732
0.20					1.106	2.377	2.000

f less than f'_m are probably too small to be of practical significance. Table I presents values of ν_x and ν_z obtained from (38) as a function of f for $N = 3$, $N = 4$, $N = 6$, and $N = \infty$. The listings for each N are terminated at the smallest f value consistent with the minima given above; the values of ν_x for $N = \infty$ are omitted since $\nu_x \equiv 1$ in this case. For a given f value, the results show that the value of N very significantly affects $(\nu_x - 1)$, but only mildly affects ν_z (except for quite small f values).

VI. DISCUSSION OF RESULTS

All the properties of the linear oscillations as a function of the energy E (expressed in m_0c^2 units) are completely determined by two geometric parameters, the number of sectors N, and the magnet fraction f; that is, these properties are independent of the rest mass and charge of the particle as well as the absolute magnetic field strength (or orbital frequency). A computer program has been developed which, for a given N and f, calculates as a function of E the most significant of these orbit properties: the horizontal and vertical focusing frequencies, ν_x and ν_z; the extreme values of the horizontal and vertical width functions listed in (34). The

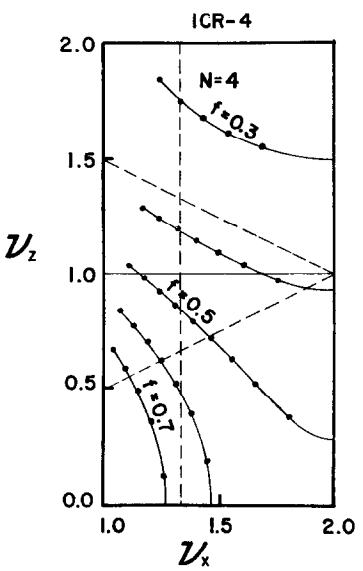

FIG. 4. Focusing frequencies for four-sector geometries. Five plots are shown of ν_z versus ν_x values for $f = 0.3, 0.4, \ldots, 0.7$ (reading from top to bottom). Blackened points are spaced at an energy interval $\Delta E = 0.05$ starting from $E = 0$ at the left. Dashed lines indicate the following resonances: $3\nu_x = 4$, $\nu_x - 2\nu_z = 0$, and $\nu_x + 2\nu_z = 4$.

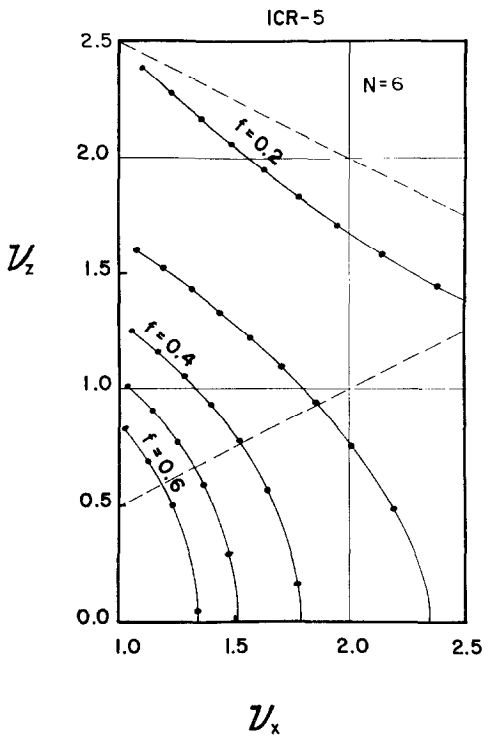

FIG. 5. Focusing frequencies for six-sector geometries. Five plots of ν_z versus ν_x values are given for $f = 0.2, 0.3, \ldots, 0.6$ (reading from the top). The blackened points are spaced at an energy interval $\Delta E = 0.1$ starting from $E = 0$ at the left. Dashed lines indicate the resonances: $\nu_x - 2\nu_z = 0$, and $\nu_x + 2\nu_z = 6$. The $f = 0.2$ curve, which is cut off at $\nu_x = 2.5$, continues until $\nu_x = 3$.

program begins at $E = 0$ and proceeds in constant ΔE steps until either $\nu_z = 0$ or $\nu_x = N/2$. The calculations are based on the formulas developed in Sections II, III, IV and assume only that the field is perfectly isochronous and that the hard-edge approximation is valid.

If g is the aperture of the magnet gap, then the validity of the hard-edge approximation requires that: $g \ll \rho\delta$, and $g \ll L = a\rho\delta$ (cf. (3)). This approximation will therefore be least reliable near injection at the lowest energies; in this case, the values of ν_z, and to a lesser extent ($\nu_x - 1$), will be lower than the corresponding hard-edge values (cf. Table I); nevertheless, the validity of the hard-edge approximation increases rapidly with energy since the value of ρ increases roughly as $E^{1/2}$. For rings with higher energy injection, the hard-edge approximation should be valid throughout.

Figures 4, 5, 6 show plots of ν_z versus ν_x for $N = 4$, 6, and 8, respectively. Each figure shows curves for five different f values: $f = 0.3(0.1)0.7$ for $N = 4$, and $f = 0.2(0.1)0.6$ for $N = 6$ and $N = 8$. The blackened points on each curve are spaced at a fixed ΔE interval starting at $E = 0$, so that the variation of ν_x and ν_z with energy is thereby indicated. These curves terminate either at $\nu_z = 0$ or at $\nu_x = N/2$, except that in Figs. 5 and 6 the drawings have been arbitrarily cut off at $\nu_x = 2.5$. Since ν_z decreases with energy while ν_x increases with energy, the slope of these curves is always negative; however, since $(d\nu_z/d\nu_x) \to 0$ as $\nu_x \to N/2$, the curvature reverses sign near the end of those curves which terminate at $\nu_x = N/2$. These figures also indicate the location of some of the "resonance lines" which are discussed below. Although they are rather striking, orbit properties for $N = 3$ will not be discussed here because these properties seem of little practical importance, except possibly for low energy cyclotrons (cf. Table I). In addition, values of $f < 0.2$ have been excluded from consideration here since such values of f would not only impose the

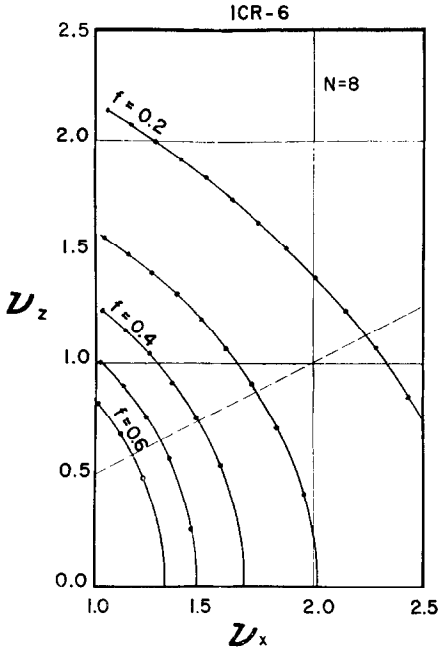

FIG. 6. Focusing frequencies for eight-sector geometries. Five plots are shown of ν_z versus ν_x values for $f = 0.2, 0.3, \ldots, 0.6$ (reading from the top). The blackened points are spaced at the constant energy interval $\Delta E = 0.1$ starting from $E = 0$ at the left. The dashed line indicates the $\nu_x - 2\nu_z = 0$ resonance. The curve for $f = 0.2$, which is cut off at $\nu_x = 2.5$, continues until $\nu_z = 0$.

TABLE II

MAXIMUM ENERGIES (in m_0c^2 units)

f	$N = 4$	$N = 6$	$N = 8$	$N = \infty$
0.2		0.91*	1.27	1.24
0.3	0.24*	0.86	0.84	0.83
0.4	0.33*	0.60	0.59	0.58
0.5	0.42*	0.43	0.42	0.41
0.6	0.31	0.30	0.29	0.29

greatest technical difficulties, but also appear unnecessary within the energy limits imposed on this type of cyclotron.

Table II presents values of the maximum energy $E_{\max}$ which can be obtained with a given f value for $N = 4$, 6, 8, and $N = \infty$. In most of the cases shown, $E_{\max}$ is reached when $\nu_z = 0$, while in the remaining cases (indicated in the table by an asterisk) $E_{\max}$ is reached when $\nu_x = N/2$. For a given value of N, the largest $E_{\max}$ is obtained for that value of f for which $\nu_z = 0$ and $\nu_x = N/2$ are reached simultaneously. The value of $E_{\max}$ represents an upper limit which cannot actually be achieved in practice since the vertical or horizontal beam width diverges when $\nu_z = 0$ or $\nu_x = N/2$, respectively. The values of $E_{\max}$ given for $N = \infty$ are obtained from (37b) by setting $\nu_{z0} = 0$.

The horizontal and vertical width functions, W_x and W_z, are defined via Eqs. (33, 21) and are given here in dimensionless cyclotron units. Since these functions specify the variation in the beam's dimensions throughout the ring, they therefore provide crucial information to the machine designer. For the vertical motion, the following relation holds:

$$\Delta z = (\Delta z_i)(W_z/W_{zi}), \tag{41}$$

where Δz is the actual beam width and W_z is the corresponding width function at a given position and energy, while Δ_{zi} and W_{zi} are the same quantities at injection (with an analogous relation between Δx and W_x). If, for example, the vertical beam aperture has a prescribed constant value throughout the ring, then the smallest value of W_{zi}/W_z within the ring will determine the largest Δz_i which can be successfully injected into the ring. If $\nu_z \ll N/2$, the value of W_{z0} obtained from Eq. (37c) provides a good estimate of the maximum width W_{ze} as a function of the energy, particularly if the correct value of ν_z is used. Thus, since the value of ν_z tends to decrease with energy faster than the value of γ increases, the value of W_{ze} generally increases with energy, and diverges as the $\nu_z = 0$ limit is approached. To compensate for this increase in W_{ze}, the vertical beam aperture could likewise

TABLE III

FOUR SECTOR ORBIT PROPERTIES

f	E	ν_x	W_{xh}	W_{xv}	ν_z	W_{zh}	W_{ze}	W_{zv}
0.3	0.00	1.245	2.486	1.218	1.840	2.591	2.610	0.625
	0.05	1.333	2.486	1.102	1.748	2.059	2.112	0.766
	0.10	1.430	2.535	0.983	1.675	1.813	1.893	0.851
	0.15	1.543	2.673	0.850	1.610	1.659	1.762	0.913
	0.20	1.689	3.065	0.679	1.548	1.550	1.673	0.965
	0.24	1.901	5.203	0.374	1.499	1.482	1.621	1.000
0.5	0.00	1.110	1.694	1.091	1.029	1.306	1.438	1.337
	0.05	1.174	1.649	1.014	0.979	1.296	1.440	1.350
	0.10	1.240	1.615	0.940	0.923	1.294	1.449	1.371
	0.15	1.310	1.594	0.868	0.862	1.299	1.467	1.400
	0.20	1.384	1.589	0.797	0.794	1.316	1.498	1.441
0.5	0.25	1.463	1.606	0.724	0.717	1.347	1.546	1.499
	0.30	1.552	1.660	0.646	0.627	1.403	1.622	1.585
	0.35	1.656	1.790	0.553	0.519	1.503	1.751	1.724
	0.40	1.798	2.212	0.414	0.376	1.724	2.022	2.006
	0.42	1.896	3.009	0.295	0.298	1.916	2.254	2.243
0.7	0.00	1.037	1.315	1.029	0.667	1.397	1.506	1.491
	0.05	1.091	1.264	0.968	0.587	1.449	1.570	1.558
	0.10	1.146	1.221	0.912	0.489	1.546	1.684	1.675
	0.15	1.202	1.183	0.859	0.360	1.758	1.924	1.918
	0.20	1.258	1.151	0.808	0.124	2.924	3.215	3.214

increase with energy; however, the increase in the isochronous field with energy tends to favor a corresponding decrease in the magnet gap towards the outside of the ring. A reasonable compromise consists in having the magnet gap and vertical beam aperture remain constant throughout the ring; moreover, such a choice clearly simplifies the construction of the machine. The increase in W_{ze} imposes limits on the feasible energy range for a given geometry; however, an increase in W_{ze} by 50 %, which could be tolerable, generally corresponds to a rather substantial energy range.

The properties of the width functions are well demonstrated by the data presented in Table III. This table displays part of the computer output for $N = 4$ with $f = 0.3$, 0.5, and 0.7. (The significance of the various W's is explained in connection with (34).) For the cases $f = 0.3$ and 0.5 the value of ν_x approaches $N/2$ at the end of the energy range, and as can be seen, the value of W_{xh} diverges, while W_{xv} approaches zero as the limiting value of ν_x is reached. The tendency for W_{xh} to

decrease in accordance with (37c) is evident only in the $f = 0.7$ case (and also at the beginning of the $f = 0.5$ case) since $\nu_x \ll N/2$ here. For $f = 0.7$ and 0.5, the value of W_{ze} tends to increase in accordance with (37c); as $\nu_z \to 0$ in these cases, the values of W_{zh}, W_{ze}, and W_{zv} tend to diverge together. In the $f = 0.3$ case, however, the value of W_{ze} initially decreases very rapidly because the value of ν_z is initially close to $N/2$; that is, whenever either ν_x or ν_z approaches $N/2$, the maximum width diverges while the minimum width decreases such that their product varies as $(f\gamma\nu)^{-1}$. An examination of this table shows that a four-sector geometry with $f = 0.5$ (depicted in Fig. 1) posesses exceptionally good orbit properties at all energies from $E = 0$ to $E = 0.3$ inasmuch as the maximum horizontal and vertical beam widths change by less than 15% over this energy range.

In order to demonstrate how the orbit properties depend on N, these properties are displayed in Table IV for $f = 0.3$ with $N = 6$, $N = 8$, and $N = \infty$. The data for $N = \infty$ are obtained from Eqs. (37a–c); in this case, $W_{x0} = W_{xh} = W_{xv}$, and $W_{z0} = W_{zh} = W_{ze} = W_{zv}$. With regard to the vertical motion, the values of W_{ze} remain nearly constant up to $E = 0.7$, and do not differ substantially in all

TABLE IV

ORBIT PROPERTIES FOR $f = 0.3$

N	E	ν_x	W_{xh}	W_{xv}	ν_z	W_{zh}	W_{ze}	W_{zv}
6	0.00	1.079	2.001	1.597	1.600	1.521	1.559	1.273
	0.20	1.316	1.724	1.282	1.434	1.413	1.473	1.264
	0.40	1.570	1.552	1.041	1.224	1.365	1.448	1.305
	0.60	1.852	1.466	0.838	0.943	1.404	1.517	1.432
	0.80	2.194	1.503	0.641	0.486	1.782	1.961	1.933
	0.86	2.321	1.568	0.574	0.182	2.842	3.145	3.139
8	0.00	1.041	1.913	1.702	1.565	1.492	1.515	1.371
	0.20	1.259	1.618	1.394	1.407	1.412	1.446	1.337
	0.40	1.482	1.412	1.170	1.200	1.391	1.437	1.359
	0.60	1.713	1.266	0.996	0.914	1.462	1.525	1.479
	0.80	1.955	1.161	0.855	0.416	2.003	2.112	2.100
	0.84	2.005	1.145	0.829	0.184	2.966	3.135	3.131
∞	0.00	1.00	1.826		1.528		1.477	
	0.20	1.20	1.522		1.376		1.421	
	0.40	1.40	1.304		1.172		1.425	
	0.60	1.60	1.141		0.879		1.539	
	0.80	1.80	1.014		0.306		2.462	
	0.82	1.82	1.003		0.145		3.558	

three cases. For the horizontal motion, the values of W_{xh} decrease monatonically in the three cases, except for the very end of the $N = 6$ case. These results contrast sharply with those for $N = 4$, $f = 0.3$ given in Table III; this contrast emphasizes the important effect of the proximity of $\nu = N/2$ on the values of the width functions. If only the variation of the W's is considered, the $f = 0.3$ geometry with $N \geqslant 6$ has excellent orbit properties up to $E = 0.7$; it may be noted, moreover, that the same conclusion holds for the $f = 0.2$ geometry up to $E = 0.8$ for $N = 6$, and up to $E = 1.1$ for $N = 8$.

VII. RESONANCES

The integral resonance $\nu_z = 1$ constitutes the most serious imperfection resonance for this type of cyclotron. Acceleration through this resonance poses very severe problems because of the postulated narrow magnet gaps. This resonance is driven by an error in the median plane field containing a radial component $\Delta B_r(\theta)$ with a first harmonic fourier component of amplitude ΔB_{r1}. Following acceleration through the $\nu_z = 1$ resonance, the beam will have developed a coherent vertical oscillation whose amplitude is given approximately by:

$$\Delta Z = \pi F[E_1 \mid d\nu_z/dE \mid]^{-1/2}, \tag{42}$$

where E_1 is the energy gain per turn, and $F = (q/p)\, r^2(\Delta B_{r1})$; a cursory examination of this formula reveals the severity of the problem. An appropriate set of coils could, in principle, be built into the ring so as to produce a corrective $\Delta B_r'$ with a harmonic of variable amplitude and azimuth which could, therefore, empirically cancel the troublesome error field otherwise present; such a mechanism could restore the beam to the median plane following the resonance. If, however, the machine is to operate with variable final energy (or with different ions), then the position of this resonance will not be fixed spatially and the design of the appropriate correcting coils would, therefore, be complicated. On the other hand, if crossing the $\nu_z = 1$ resonance is to be avoided, then the values of ν_z throughout the ring must be restricted to either $\nu_z < 1$ or $1 < \nu_z < 2$. As can be seen from Figs. 4–6, such a restriction limits the choice of admissible f values, or limits the feasible energy range for a particular f value. For values of $f \gtrsim 0.5$, the values of ν_z remain below $\nu_z = 1$ at all energies, and this restriction on f seems appropriate for low energy cyclotrons. For the $f = 0.3$ geometries whose orbit properties are given in Table IV, the values of ν_z remain above $\nu_z = 1$ at all energies up to $E = 0.54$, which would then become the energy limit for these geometries. As a further example, for $N = 8$ and $f = 0.2$, the requirement that $1 < \nu_z < 2$ restricts the available energy range from $E = 0.2$ to $E = 1.0$.

Unlike the conventional isochronous cyclotron, the design considered here

effectively avoids the difficulties associated with the $\nu_x = 1$ resonance at low energies since, as can be seen from Table I, the values of $(\nu_x - 1)$ are significantly above zero at $E = 0$ for values of f of practical interest. For $N = 4$ geometries the $\nu_x = 2$ resonance represents the stopband limit and must be carefully avoided (cf. Table III). For $N \geqslant 6$ geometries, the $\nu_x = 2$ resonance does not occur except for small f values; for $N = 6$, the $\nu_x = 2$ resonance occurs at $E = 0.63$ for $f = 0.2$, and at $E = 0.70$ for $f = 0.3$; for $N = 8$, this resonance occurs at $E = 0.80$ for $f = 0.2$, and at $E = 0.83$ for $f = 0.3$. The coherent horizontal oscillation induced by acceleration through the $\nu_x = 2$ resonance can be used to facilitate beam extraction for $N \geqslant 6$, provided that this resonance can actually be reached within the limitations imposed by other considerations.

The half-integral imperfection resonances $\nu_y = n/2$ (e.g., $\nu_x = 3/2$, $\nu_z = 1/2$ or $3/2$) should pose far less serious problems than those presented by the integral resonances. Acceleration through a half-integral resonance can produce only an increase in the effective phase space area occupied by the beam, and if suitable precautions are taken, this increase will be minimal. If an error $\Delta k(\theta)$ exists in the field index having a nth fourier harmonic of amplitude Δk_n, then the value of ν_y in the vicinity of the resonance will be changed to ν_y^* given by the approximate formula:

$$(\nu_y^* - n/2)^2 = (\nu_y - n/2)^2 - [(\Delta k_n)/2n]^2. \tag{43}$$

Thus, for a range of energies in the neighborhood of $\nu_y = n/2$, the value of ν_y^* will have an imaginary component (stop-band); the duration and strength of this imaginary component are each proportional to Δk_n. If the incoherent oscillations within the beam prior to the resonance are characterized by a maximum amplitude A (cf. Eq. (21)), then after acceleration through the resonance, this amplitude will be increased by ΔA given approximately by:

$$\Delta A = A[\pi(\Delta k_n)/2n]^2 \, [E_1 \mid d\nu_y/dE \mid]^{-1}. \tag{44}$$

With proper care it should be possible to achieve $(\Delta A)/A < 0.1$, in which case the half-integral resonance traversal would not represent a serious barrier. The one situation to be avoided is where ν_z starts out at low energy close to $1/2$ or $3/2$ and then hovers about this value over an appreciable energy range because of a failure in the hard-edge approximation.

For $N = 4$ geometries, the essential third-order (in the Hamiltonian) resonance $\nu_x = 4/3$ frequently occurs within a desirable energy range as can be seen in Fig. 4 and Table III. For the narrow gap magnets of constant angular width being considered here, the fourier component $B_4(r) \cos 4\theta$ of the median plane field increases rather slowly with radius (this increase being almost entirely produced by the isochronism requirement); consequently, the nonlinear driving force for the $\nu_x = 4/3$

resonance is exceptionally weak, so that acceleration through this resonance should produce only an insignificant distortion of the beam's phase space area. This situation contrasts markedly with that obtaining in spiral-ridge magnets, where the spiralling produces very strong nonlinear forces. This situation also differs substantially from that obtaining in the ORNL four-sector electron cyclotron (*5*); although that cyclotron had radial sectors, since the field contained only a few fourier components, the value of $B_4(r)$ was forced to increase rapidly with radius in order to produce adequate vertical focusing throughout the machine; by contrast, the magnet structure considered here has a large number of strong fourier components contributing significantly to the vertical focusing. For $N = 6$ configurations, the $\nu_x = 6/3$ resonance coincides with the $\nu_x = 2$ resonance, and contributes to the effects of the latter (discussed above) only if large amplitudes are generated in traversing this resonance. The fourth-order essential resonance $\nu_x = N/4$ (e.g. 6/4 or 8/4) poses even less of a problem than the $\nu_x = N/3$ resonance. The corresponding essential resonance $\nu_z = N/4$ (in particular, 4/4 or 6/4) in the vertical motion should produce no difficulties provided, as must be required, the vertical extent of the beam is sufficiently small compared to the magnet gap so that the vertical motion is essentially linear throughout.

Among the essential nonlinear coupling resonances, those requiring the greatest attention are the third-order resonances: $\nu_x + 2\nu_z = N$, $\nu_x - 2\nu_z = 0$; and to a lesser extent the fourth-order resonances: $2\nu_x + 2\nu_z = N$, $2\nu_x - 2\nu_z = 0$; while the higher order resonances are again presumably neligible. Furthermore, the linear imperfection resonances $| \nu_x \pm \nu_z | = n$ should also be investigated. In plots of ν_z versus ν_x the "difference" resonances and the "sum" resonances appear as lines having positive and negative slopes, respectively; to avoid clutter, only the third-order essential resonances are shown in Figs. 4–6 insofar as these resonance lines fall within the given boundaries of the drawings. The nonlinear resonances should be relatively weak since the only strong field gradient occurs across the magnet edge, and this gradient varies slowly with radius; as a result, if the beam is reasonably well-centered on the equilibrium orbit, then acceleration through a nonlinear coupling resonance should proceed without significant damage, provided the resonance is traversed fairly rapidly. This proviso is clearly fulfilled by the difference resonances since the slopes of these resonance lines are opposite in sign to that for the ν_z versus ν_x curve of the accelerating particles. With regard to the sum resonances, however, for certain values of f the ν_z versus ν_x curves closely parallel resonance lines. Obviously, such a situation invites potentially disasterous results and should be strictly avoided; as a consequence, for a given value of N, certain values of f should be definitely excluded from consideration.

For $N = 4$, the $\nu_x + 2\nu_z = 4$ resonance is the most serious coupling resonance, and this line falls between the curves for $f = 0.36 - 0.37$ such that $| \nu_x + 2\nu_z - 4 | < 0.07$ at all energies up to $E = 0.25$, and such values of f

must therefore be excluded; however, the $f = 0.4$ curve has $| \nu_x + 2\nu_z - 4 | > 0.25$ at all energies, and should be quite acceptable. For $N \geqslant 6$, the $\nu_x + 2\nu_z = N$ resonance line does not come close to the ν_z versus ν_x curves for $f \geqslant 0.2$ (cf. Figs. 5-6). For $N = 4$, the $2\nu_x + 2\nu_z = 4$ resonance line (which coincides with $\nu_x + \nu_z = 2$) is closely bracketed by the curves for $f = 0.55 - 0.56$ at all energies up to $E = 0.2$, and values of f in this vicinity should also be excluded; however, the $f = 0.5$ curve has $2\nu_x + 2\nu_z > 4.28$ over its entire energy range, and should therefore be acceptable. For $N = 6$, the $2\nu_x + 2\nu_z = 6$ (or $\nu_x + \nu_z = 3$) resonance line should exclude values of f close to $f = 0.26 - 0.27$, since the curves for these f values closely parallel the resonance line at all energies up to $E = 0.6$; however, the curve for $f = 0.3$ is satisfactory since $2\nu_x + 2\nu_z < 5.6$ in this case over the entire useful energy range. For $N \geqslant 8$, the $2\nu_x + 2\nu_z = N$ resonance line does not appear close to the ν_z versus ν_x curves for values of f considered important here. The linear imperfection resonances are presumably less serious since they can, in principle, be counteracted by appropriate measures; nevertheless, these resonances should be avoided if possible. It is therefore worth noting that for $N \geqslant 6$, the $\nu_x + \nu_z = 2$ resonance line closely parallels the curves for $f = 0.51 - 0.52$ at the interesting energies; moreover, the $\nu_x + \nu_z = 3$ resonance line is bracketed by the curves for $f = 0.30 - 0.32$ for $N = 4$, and is crossed twice by curves with $f \cong 0.24$ for $N = 8$.

The foregoing discussion represents only a general survey of the various resonances encountered in this type of cyclotron; these resonances should be investigated more thoroughly when a specific geometry is being given serious study. Considering the limitations imposed by all the resonances, the four-sector geometry with $f = 0.5$ has very good orbit properties at all energies up to about $E = 0.3$ (cf. Fig. 1 and Table III); moreover, studies carried out at Indiana University show that for this geometry the values of ν_z actually lie below $\nu_z = 1$ at low energies due to the failure of the hard-edge approximation. The six-sector geometry with $f \cong 0.3$ posesses desirable orbit properties and avoids resonance difficulties at all energies up to about $E = 0.5$ (cf. Fig. 2 and Table IV). Many other configurations also appear promising, particularly for rings operating within a restricted energy range.

The present analysis has considered only one possible arrangement of magnet sectors consisting of "wedge-shaped" magnets. The general arrangement for wedge-shaped magnets can be defined by three parameters: (a), the angular width of the wedge; (b), the displacement (positive or negative) of the apex of the wedge from the machine center; and (c), the angle between this displacement and the line bisecting the wedge. The present paper has explored only those cases for which the parameters (b) and (c) are both equal to zero. Other symmetric configurations can be obtained by varying the parameter (b) while retaining the parameter (c) equal to zero. If both of these parameters are different from zero, then the geometry becomes asymmetric and posesses some of the attributes of spiralled magnet sectors.

In addition, a sector could contain more than one wedge-shaped magnet. All these possibilities remain to be investigated.

This paper is indirectly an outgrowth of a previous paper which presented, among other topics, a qualitative discussion of a 200 MeV Isochronous Cyclotron Ring with radial sectors (*2*). Some of the ideas expressed in that paper have been suitably modified and extensively developed for use in the proposed 200 MeV cyclotron being designed at Indiana University. It was as a result of my interaction with Martin Rickey and Bryce Bardin at Indiana University that the work described in the present paper was conceived and carried out. I am therefore indebted to these people for fruitful discussions and for their encouragement of this work.

RECEIVED: July 1, 1968

REFERENCES

1. J. P. BLASER AND H. A. WILLAX, *IEEE Trans. Nucl. Sci.* NS-**13**, 194 (1966).
2. M. M. GORDON, *Nucl. Instr. and Meth.* **58**, 245 (1968).
3. J. J. LIVINGOOD, "Principles of Cyclic Particle Accelerators," Chapter 4. D. Van Nostrand, Princeton, 1961.
4. E. D. COURANT AND H. S. SNYDER, *Ann. Phys.* **3**, 1 (1958).
5. BLOSSER, WORSHAM, GOODMAN, LIVINGSTON, MANN, MOSELEY, TRAMMEL, AND WELTON, *Rev. Sci. Instr.* **29**, 819 (1958).